Hindawi
Geofluids
Volume 2022, Article ID 9159242, 10 pages
https://doi.org/10.1155/2022/9159242

Research Article

Digital Core Modeling Based on Pretrained Generative Adversarial Neural Networks

Qing Zhang, Benqiang Wang, Xusheng Liang, Yizhen Li, Feng He, and Yuexiang Hao

Shale Gas Exploration and Development Project Management Department of CNPC Chuanqing Drilling Engineering Company Limited, Chengdu 610051, China

Correspondence should be addressed to Benqiang Wang; wangbq_cqyyq@cnpc.com.cn

Received 24 May 2022; Accepted 17 August 2022; Published 5 September 2022

Academic Editor: Dengke Liu

Accurately establishing a 3D digital core model is of great significance in oil and gas production. The physical experiment method and numerical modeling method are common modeling methods. With the development of deep learning technology, a variety of deep learning algorithms have been applied to digital core modeling. The digital core modeling method based on generative adversarial neural networks (GANs) has attracted wide attention due to its good quality and simple generation process. The disadvantage of this method is that the network needs thousands of trainings to achieve acceptable results. For this reason, this paper proposes to use the pretrained GANs for digital core modeling training, which can greatly reduce the number of network training while ensuring the core modeling effect. We can use the presented method to quickly complete the training and use the trained generator model to obtain multiple digital cores. By analyzing the quality of the generated cores from multiple aspects, it is revealed that the properties of the generated cores are in good agreement with the ones of the real core samples. The results indicate the reliability of the pretrained GAN method.

1. Introduction

In order to find and exploit oil and gas reservoirs better, the demand for fine reservoir characterization is constantly increasing [1, 2]. It is of great significance to find a method that can accurately describe the internal structure of complex rocks [3]. With the development of computers and various scanning imaging technologies, the digital core technology that reflects the internal microstructure of rocks with 3D digital images has developed rapidly [4]. The digital core can accurately reflect the spatial structure inside the rock [5] and carry out the simulation of rock electrical characteristics [6–10], elastic properties [11–15], seepage characteristics, and NMR simulation response [16–20] and obtain a variety of physical properties of the rock for better reservoir evaluation. The physical experiment method and numerical reconstruction method are currently commonly used digital core modeling methods [21]. The physical experiment method uses a scanning imaging instrument to obtain multiple 2D images of cores and then obtains 3D core images through mathematical algorithms. The physical experiment method mainly includes the sequence slice superposition method [22], X-ray CT scanning method [23, 24], and focused ion-scanning electron double beam microscope method [25]. The digital core model obtained by the physical experiment methods can accurately describe the internal structure and mineral composition of the rock. The disadvantage is that it requires professional equipment and software, and the high cost limits the wide use of this method. Considering the cost, using core analysis data and 2D thin slices for digital core modeling is a good choice. Numerical reconstruction methods include stochastic simulation method and process-based method. The stochastic simulation method obtains information from the 2D rock images as constraint conditions to establish a digital core model, including the random Gaussian field method [26],

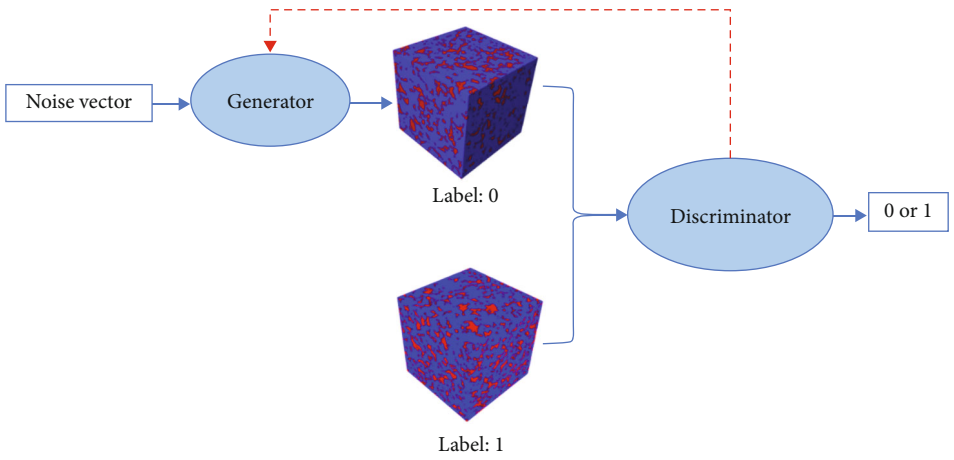

Figure 1: Model structure diagram.

Table 1: Network structure parameter table.

	Layer	Type	Convolution kernel	Stride	Padding	Normalized	Activation function
Generator	1	ConvTransp3D	(256,4,4,4)	1	0	Yes	ReLU
	2	ConvTransp3D	(128,4,4,4)	2	1	Yes	ReLU
	3	ConvTransp3D	(64,4,4,4)	2	1	Yes	ReLU
	4	ConvTransp3D	(32,4,4,4)	2	1	Yes	ReLU
	5	ConvTransp3D	(1,4,4,4)	2	1	No	Tanh
Discriminator	1	Conv3D	(16,4,4,4)	2	1	No	LeakyReLU
	2	Conv3D	(32,4,4,4)	1	1	Yes	LeakyReLU
	3	Conv3D	(64,4,4,4)	1	1	Yes	LeakyReLU
	4	Conv3D	(128,4,4,4)	1	1	Yes	LeakyReLU
	5	Conv3D	(1,4,4,4)	1	0	Yes	Sigmoid

simulated annealing method [27], Markov Chain-Monte Carlo Method [28], and multiple point statistics method [29]. The process-based method determines the radius of sedimentary particles through rock particle size analysis data, simulates the formation process of rocks, and establishes a 3D digital core model [30]. When using the above-mentioned numerical methods for digital core modeling, it is necessary to manually select various characteristic functions and constraint conditions, and it is necessary to repeat the complete process many times when digital core modeling. Generally, as the size of the generated core increases, the amount of calculation required for modeling also increases exponentially.

With the rapid development of deep learning research, generative learning using the powerful feature extraction and expression capabilities of neural networks has become a research hotspot. The convolutional neural network has a wide range of applications in image processing under the characteristics of local connection and weight sharing [31, 32]. As a typical unsupervised learning model, autoencoders are widely used in image editing and generation [33]. Goodfellow et al. proposed the generative adversarial neural networks (GANs) in 2014. The proposal of this network has greatly promoted the research in the field of unsupervised learning and image generation [34]. The digital core is used as a 3D digital image, and a variety of deep learning algorithms have achieved good results in digital core modeling. Mosser et al. used DCGANs to achieve rapid modeling of a variety of digital cores, and the obtained core samples are in good agreement with the real core samples [35, 36]. Valsecchi et al. used DCGANs to generate 3D digital cores from 2D images of rocks, which is fast and accurate [37]. Zha et al. used WG-GANs to generate high-quality shale pictures, which are consistent and diverse with real shale samples [38]. Feng et al. used CGANs to obtain a complete core image from a limited image [39]. Many researchers combined AE and GANs to realize the generation of 3D digital core from 2D core thin slices [40, 41]. Feng et al. used Bicycle GANs to realize the process from 2D core slicing to 3D digital core reconstruction [42]. Wang et al. used the CNN network to achieve high-resolution 3D digital core modeling [43]. Ong et al. proposed generative encoding in combination with GANs and AE, which realized the use of 2D slices to generate 3D digital cores [44]. Compared with traditional numerical modeling methods, the use of deep learning algorithms can save researchers from paying too much attention to the extraction of feature information, and the training process is relatively simple. The parameters obtained during

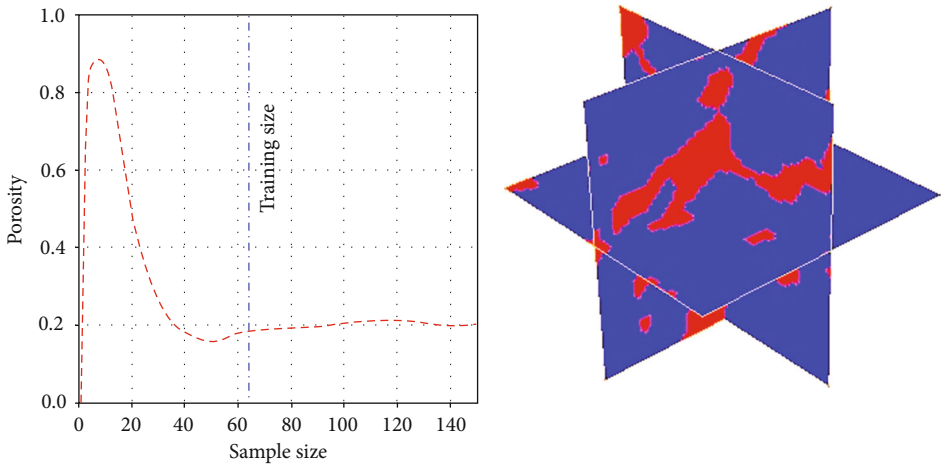

(a) REV analysis results (b) REV section view

FIGURE 2: Representative volume element analysis and schematic diagram of Berea sandstone.

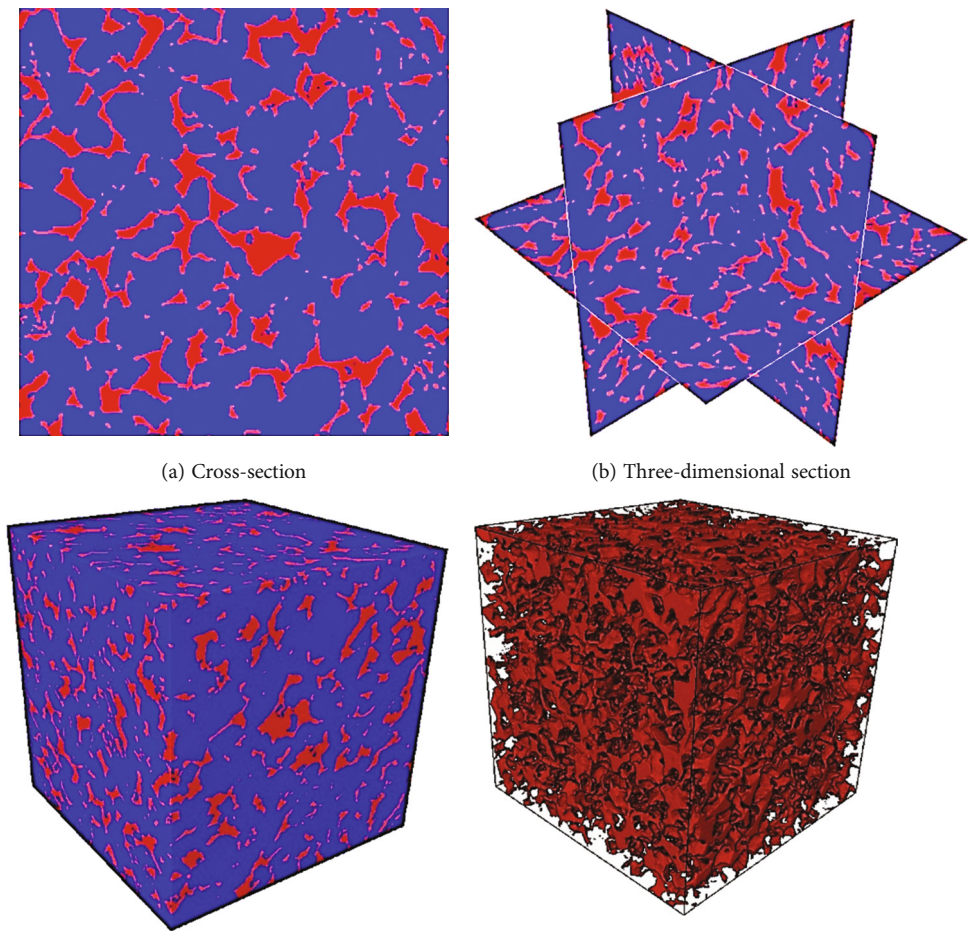

(a) Cross-section (b) Three-dimensional section

(c) Outer surface (d) Pore structure

FIGURE 3: Real core images.

the training process can be saved, and the subsequent core reconstruction process can be directly completed quickly using the parameters obtained during the training.

Previous studies have shown that high-quality digital core models can be obtained by using network models that generative adversarial neural networks and its variants.

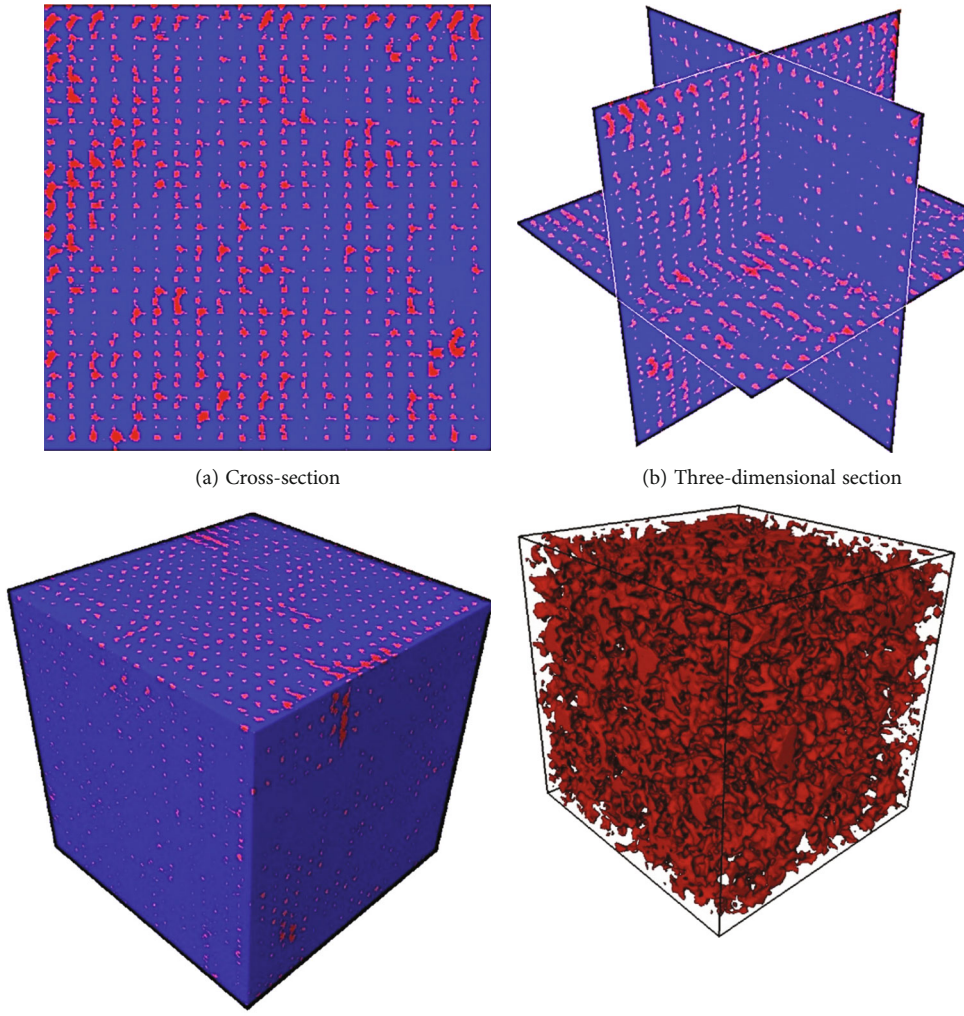

(a) Cross-section (b) Three-dimensional section

(c) Outer surface (d) Pore structure

Figure 4: Digital core modeling based on no pretrained GANs.

However, the training of GANs is a complicated process, and it is easy to encounter problems such as gradient disappearance or mode collapse during the training process [38]; it usually takes thousands or even tens of thousands of training times to achieve a better generation effect. Therefore, it is of great significance to find a way to effectively reduce the number of trainings of GANs. This paper is based on the DCGAN model proposed by Radford et al. [45], using the pretrained GANs for digital core generation training can effectively reduce the number of network training while ensuring the quality of the generated core samples. The follow-up arrangement of the paper is as follows: in the second part, the structure of the generative adversarial neural networks and the parameter setting of the training process of this paper are introduced; the training data and training process are shown in the third part, and the generation effect of the model is analyzed. The fourth part elaborates the conclusions obtained in this paper.

2. Methods

2.1. GANs. GANs are mainly composed of two parts, the generator network (G) and the discriminator network (D), which are in a state of confrontation during training [34]. The goal of the generator is to learn the data distribution characteristics of real samples and generate fake samples with a high degree of similarity to real samples, so that the discriminator cannot distinguish the authenticity of the input samples. The goal of the discriminator is to accurately distinguish the input samples from the real training samples or fake samples from the generator. As the number of training increases, the capabilities of the generator and the discriminator continue to improve. Eventually reaching a balance between the generator and discriminator, that is, when the discriminator has a strong discriminatory ability but cannot correctly determine the source of the data, a generator network model that can generate samples that conform to the characteristic distribution of real data is obtained. The generator takes a random vector as input and outputs the generated pseudo samples. The discriminator takes real samples and pseudo samples from generator as input and outputs 0 and 1. The output result is 0 for pseudo samples and 1 for real samples. According to the loss function of the discriminator and the generator, the gradient descent method is used to update the parameters of the

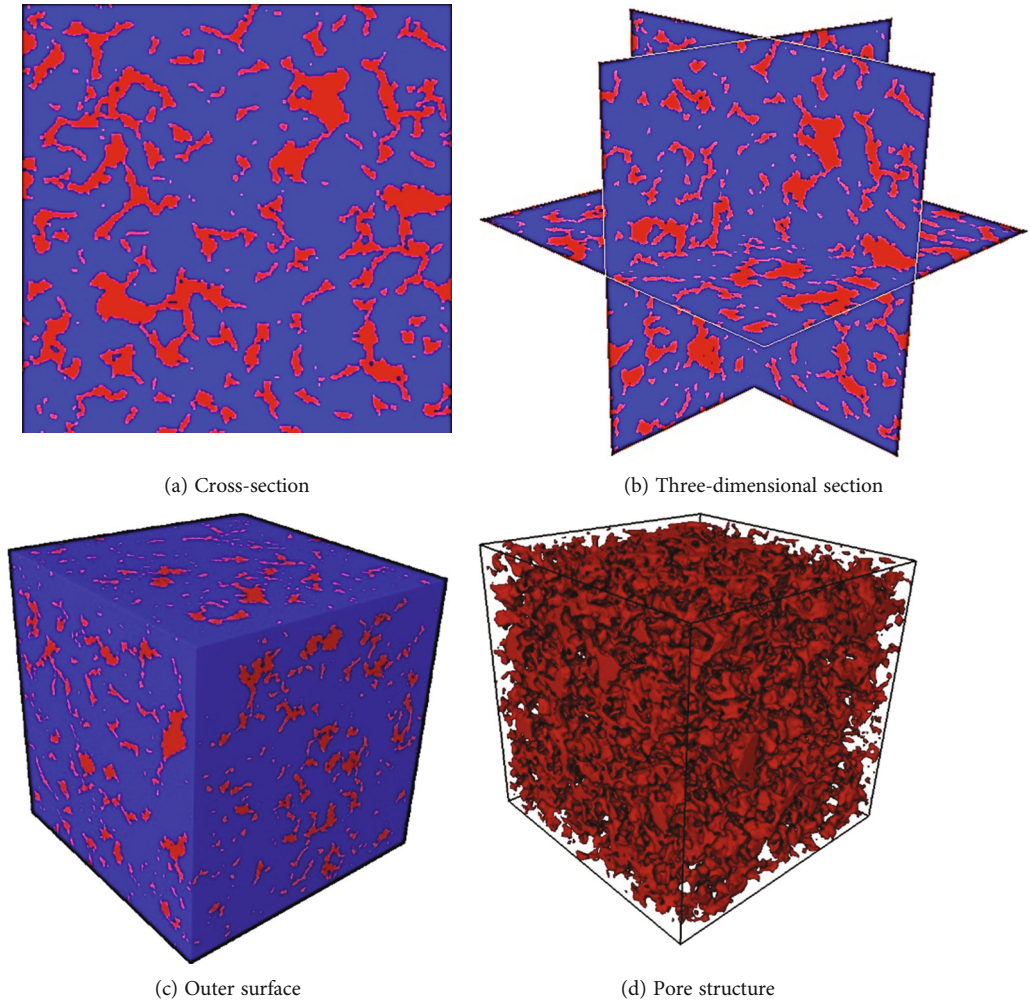

(a) Cross-section (b) Three-dimensional section

(c) Outer surface (d) Pore structure

Figure 5: Digital core modeling based on pretrained discriminator.

Table 2: Comparison of parameters between real core sample and generated core samples.

Samples	Porosity (%)	Specific area (μm^{-1})
Real core sample	19.65	0.438
Generated sample 1	19.51	0.387
Generated sample 2	19.68	0.384
Generated sample 3	19.50	0.389
Generated sample 4	19.52	0.386
Generated sample 5	19.55	0.385

network in the training of the generated confrontation neural network, so as to achieve the purpose of optimizing the network parameters of the model. The following will briefly introduce the optimization function of GANs:

$$\min_{G}\max_{D} V(G,D) = E_{x\sim p_r}[\log(D(x)] + E_{x\sim p_g}[\log(1-D(x))], \tag{1}$$

where $x \sim p_r$ represents the real sample and $x \sim p_g$ represents the pseudo sample generated by the generator. When optimizing the parameters of the discriminator, keep the generator parameters fixed. The objective function of the discriminator consists of two parts: (1) for all real samples, the discriminator should judge them as true samples, so that $D(x)$ is 1, which maximizes $E_{x\sim p_r}[\log(D(x)]$; (2) for the pseudo sample from the generator, the discriminator judges it as a pseudo sample, makes $D(x)$ 0, and maximizes $E_{x\sim p_g}[\log(1-D(x))]$, that is to maximize $V(G,D)$. Generate parameter optimization, fix the parameters of the trained discriminator, and optimize the parameters of the generator$G(z;\theta)$. The goal of generator optimization parameters is to make the discriminator judge the output of the generator as a true sample; let $D(x)$ be 1, which minimizes $E_{x\sim p_g}[\log(1-D(x))]$. It can be seen from the training of GANs that the parameter update information of the generator comes from the result of the discriminator; that is, the distance between the data distribution and the model distribution is obtained by neural network fitting, which avoids the solution of the sample probability density function.

2.2. Network Structure and Parameter Setting. The pretrained generative adversarial neural network model

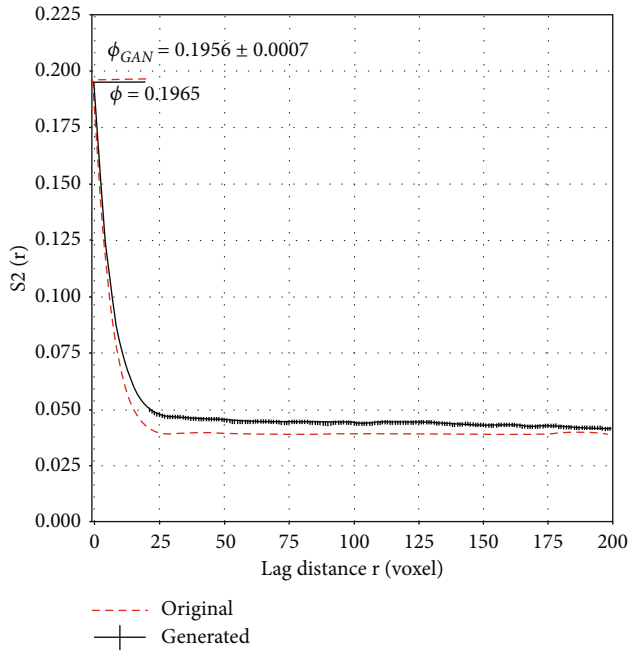

Figure 6: Radial covariance functions of generated core samples and training sample.

proposed in this paper is used for digital core modeling. The network structure is shown in Figure 1.

In training, the generator $G(z;\theta)$ through 5 transposed convolutional layers, a random noise z in a latent space is mapped to the image domain to generate a three-dimensional digital core. d is the dimension of random noise, which is set to 512 in this paper, and $N(0,1)$ represents a standard normal distribution with a mean value of 0 and a standard deviation of 1.

$$z \sim N(0,1)^{d\times 1\times 1\times 1}, \tag{2}$$

$$G_\theta : z \longrightarrow R^{64\times 64\times 64}. \tag{3}$$

The discriminator $D(x;\varphi)$ maps the real core samples and the generated core samples to the interval [0,1] through 5 convolutional layers to complete the sample determination:

$$D_\varphi : R^{64\times 64\times 64} \longrightarrow [0,1]. \tag{4}$$

The network structure parameters of the generator and the discriminator are shown in Table 1.

3. Digital Core Modeling

3.1. Sample Data and Training Process. The selected training data is the Berea sandstone X-CT scan sample of Imperial College London, the sample size is 400^3 voxels, and the resolution is 3 μm/voxel [46]. The sample image has been thresholded and only contains pores and skeleton parts. In order to ensure the number of training samples and reduce the amount of calculation in the model training process, the porosity is used as a constraint to find the representative volume element that can reflect the nature of the original sample. Figure 2(a) shows the variation of porosity with the size of the subsample. It can be seen that when the side length of the training sample is greater than 60 voxels, the porosity gradually stabilizes. Therefore, the training sample is set as a cube with a side length of 64 voxels, the sample interval is 32 voxels, and a total of 1331 subsamples are obtained. Figure 2(b) is a three-dimensional section view of an arbitrarily selected representative volume element.

Previous scholars used generative adversarial neural networks to model digital cores and directly carried out network training on the basis of all training data. In the beginning, both the generator network and the discriminator network are networks initialized with parameters, and the latter two always keep the same training times until the generator network can obtain satisfactory results, and the training of the network is ended. The changes in this paper are mainly in the network training process. The specific process of using the pretrained generative adversarial neural networks for digital core modeling proposed in this paper is as follows:

(1) Randomly select 300 subsamples from the training sample as sample data for network pretraining, set the learning rate to 0.0003 and batch size to 16, use the Adam optimizer, and set the momentum to 0.5. There is no need to pay attention to the quality of the network during pretraining, so you can train hundreds of times. The number of pretrainings in this paper is set to 300

(2) After the pretraining is completed, use the discriminator pretrained 300 times to train the network. At this time, the generator in the network is initialized with parameters, and the discriminator is trained a certain number of times. Use the divided 1331 subsamples as training data and set the learning rate to 0.0005, batch size to 32, optimizer to Adam, and momentum to 0.5 to start network training. Through many experiments, it is found that when training 800 times, the model can achieve a better generation effect. At the same time, it is found that when the network model achieves a good generation effect using this method, continued training may cause the generation effect to deteriorate

3.2. Comparison of Modeling Effects. We implemented the training of digital core modeling with both the method presented in this paper and the previous methods, keeping the same training parameters and training times, and used the generator obtained by training 800 times to generate some digital core models of the same size as the original training core sample. A comparative analysis of the modeling effects of digital cores is carried out in various aspects.

3.2.1. Image Appearance Comparison. The cross-section, three-dimensional section, outer surface, and pore structure of the generated sample and the real sample are compared and analyzed. Figure 3 is a list of images of the real sample,

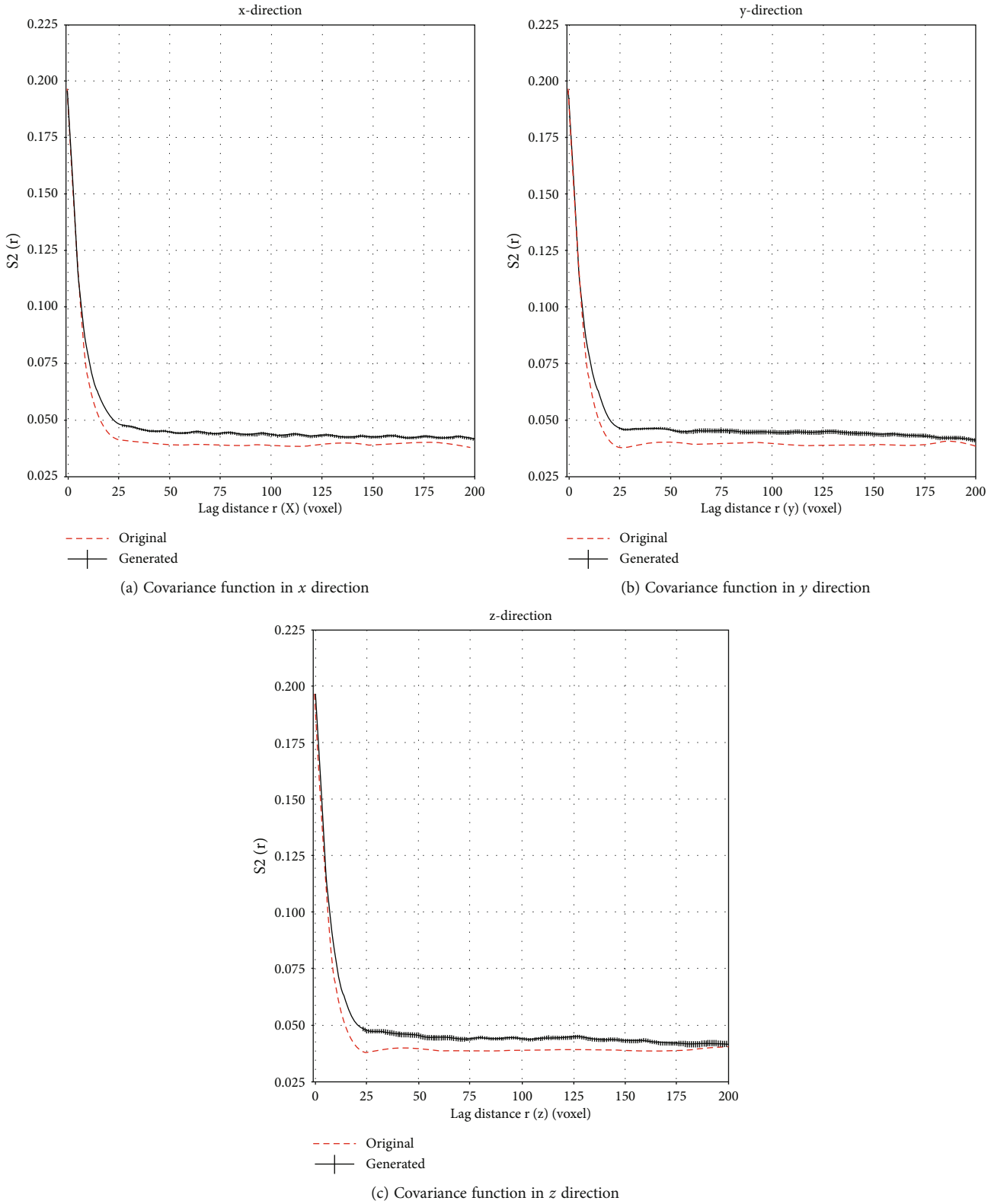

(a) Covariance function in x direction

(b) Covariance function in y direction

(c) Covariance function in z direction

Figure 7: Comparison of covariance functions in x, y, and z directions.

Figure 4 is a list of core images obtained by normal training 800 times, and Figure 5 is a list of core images obtained by using a pretrained discriminator. It can be seen that using the pretrained discriminator, after the network model is trained 800 times, the pore shape and pore distribution have good consistency with the original training sample, and there is good connectivity between the pores, indicating the core generation effect better. Without pretraining, the core

generated after 800 training is very different from the original training sample in terms of pore shape, distribution, and connectivity, indicating that the quality of the generated core is poor. It can be seen intuitively from the appearance that the generation effect of the neural network model without pretraining is very poor, so in the subsequent analysis, the digital core model obtained by the non-pretraining neural network is not analyzed.

3.2.2. Morphological Parameters. Porosity and specific surface area are common morphological parameters in core comparison, which can quantitatively evaluate the morphological characteristics of cores. Porosity is used to reflect the degree of pore development of the rock and is the ratio of the sum of the volume of pore spaces in the rock to the total volume of the rock sample. The specific surface area refers to the ratio of the total area of the pores in the core to the total volume, which is a parameter related to the pore size. Randomly select 5 digital cores obtained by using the pretrained generative adversarial neural network, and calculate the porosity and specific surface area of these cores and the original cores. The calculation results are shown in Table 2. It can be seen from Table 2 that the porosity and specific surface area of the generated core are very close to the real sample, indicating that the generated core samples are close to the training samples in nature, and the model generation effect is better.

3.2.3. Two-Point Covariance Function. The two-point covariance function $S_2(r)$ can be used to characterize the spatial structure of the core. The two-point covariance function can be expressed as follows:

$$S_2(r) = P(x \in P, x + r \in P) \quad x, r \in R^d. \tag{5}$$

That is, the probability is that the two points x and $x + r$ separated by the separation distance r are located in the pore phase P. At the origin, $S_2(0)$ is equal to the porosity $\varnothing$; when $r \longrightarrow \infty$, $S_2(r)$ will stabilize at $\varnothing^2$. Since the core is anisotropic, we calculate the $S_2(r)$ of the training sample and the generated digital core along the x, y, and z coordinate axis directions and the radial average to evaluate the effect of the model.

Figures 6 and 7 are the comparison of radial covariance functions and covariance functions in x, y, and z directions, respectively. It can be seen from the figures that the covariance function of the generated core samples and the training sample in the radial direction and the x, y, and z directions has a good consistency, indicating that the spatial structure of the generated lithology is close to the training sample.

4. Conclusions

In order to solve the problem of tens of thousands of times required for digital core generation training of the generative adversarial neural networks, this paper proposes a pretrained discriminator to train the digital core modeling of the generative adversarial neural network. The method proposed in the paper was used to train the network about 800 times, and a number of digital core models were generated. Through various analyses of the generated core samples, the following conclusions can be drawn:

(1) Comparing generated cores and real core from visual and quantitative analysis, it can be seen that the generated digital cores have good consistency with the real core, which proves that the use of generative adversarial neural networks can generate high-quality digital core models

(2) The method in this paper can achieve a good modeling effect in about 800 network trainings, which proves the reliability of the method. Under the premise of ensuring the effect of model generation, the training times of the network can be greatly reduced, thereby greatly shortening the training time of the network

Data Availability

The data that support the findings of this study are available from the corresponding author upon reasonable request.

Conflicts of Interest

The authors declare that they have no conflicts of interest.

References

[1] D. Ren, L. Ma, D. Liu, J. Tao, X. Liu, and R. Zhang, "Control mechanism and parameter simulation of oil-water properties on spontaneous imbibition efficiency of tight sandstone reservoir," *Frontiers in Physics*, vol. 10, article 829763, 2022.

[2] D. Ren, H. Zhang, Z. Wang, B. Ge, D. Liu, and R. Zhang, "Experimental study on microscale simulation of oil accumulation in sandstone reservoir," *Frontiers in Physics*, vol. 10, article 841989, 2022.

[3] C. H. Arns, H. Averdunk, F. Bauget et al., *Digital core laboratory: analysis of reservoir core fragments from 3D images*, SPWLA 45th Annual Logging Symposium. OnePetro, 2004.

[4] M. J. Blunt, B. Bijeljic, H. Dong et al., "Pore-scale imaging and modelling," *Advances in Water Resources*, vol. 51, pp. 197–216, 2013.

[5] J. Zhao, H. Chen, N. Li, J. Ding, and J. Gao, "Research advance of petrophysical application based on digital core technology," *Progress in Geophysics*, vol. 35, pp. 1099–1108, 2020.

[6] E. Garboczi, "Finite element and finite difference programs for computing the linear electric and elastic properties of digital images of random materials," *Rep 6269. NIST Interagency/Internal Report (NISTIR)*, vol. 6269, p. 198, 1998.

[7] L. Jiang, J. Sun, X. Liu, and H. Wang, "Study of different factors affecting the electrical properties of natural gas reservoir rocks based on digital cores," *Journal of Geophysics and Engineering*, vol. 8, no. 2, pp. 366–371, 2011.

[8] X. Liu, J. Sun, and H. Wang, "Numerical simulation of rock electrical properties based on digital cores," *Applied Geophysics*, vol. 6, no. 1, pp. 1–7, 2009.

[9] C. Li, F. Hu, Y. Hou, X. Li, X. Liu, and C. Li, "Simulation of electrical resistivity characteristics of tight sands reservoir by

FEM," *Shiyou Xuebao/Acta Petrolei Sinica*, vol. 37, pp. 787–795, 2016.

[10] X. Nie, C. C. Zou, X. H. Meng, S. Jia, and Y. Wan, "3D digital core modeling of shale gas reservoir rocks: a case study of conductivity model," *Natural Gas Geoscience*, vol. 27, pp. 706–715, 2016.

[11] A. P. Roberts and E. J. Garboczi, "Elastic properties of model random three-dimensional open-cell solids," *Journal of the Mechanics and Physics of Solids*, vol. 50, no. 1, pp. 33–55, 2002.

[12] A. P. Roberts and E. J. Garboczi, "Computation of the linear elastic properties of random porous materials with a wide variety of microstructure," *Proceedings of the Royal Society A: Mathematical, Physical and Engineering Sciences*, vol. 458, no. 2021, pp. 1033–1054, 2002.

[13] E. H. Saenger and T. Bohlen, "3D finite-difference modeling of viscoelastic and anisotropic wave propagation using the rotated staggered grid," *Geophysics*, vol. 69, no. 2, pp. 583–591, 2004.

[14] A. B. Andhumoudine, X. Nie, Q. Zhou et al., "Investigation of coal elastic properties based on digital core technology and finite element method," *Advances in Geo-Energy Research*, vol. 5, no. 1, pp. 53–63, 2021.

[15] X. Y. Yin, Q. P. Qin, and Z. Y. Zong, "Simulation of elastic parameters based on the finite difference method in digital rock physics," *Acta Geophysica Sinica*, vol. 59, pp. 3883–3890, 2016.

[16] S. Bakke and P. E. Øren, "3-D pore-scale modelling of sandstones and flow simulations in the pore networks," *SPE Journal*, vol. 2, no. 2, pp. 136–149, 1997.

[17] J. F. Guo, R. H. Xie, and Y. Ding, "Numerical simulation of multi-dimensional NMR response in tight sandstone," *China Sciencepaper (in Chinese)*, vol. 13, no. 3, pp. 285–294, 2016.

[18] H. Okabe and M. J. Blunt, "Prediction of permeability for porous media reconstructed using multiple-point statistics," *Physical Review. E, Statistical Physics, Plasmas, Fluids, and Related Interdisciplinary Topics*, vol. 70, p. 10, 2004.

[19] T. Ramstad, N. Idowu, C. Nardi, and P. E. Øren, "Relative permeability calculations from two-phase flow simulations directly on digital images of porous rocks," *Transport in Porous Media*, vol. 94, no. 2, pp. 487–504, 2012.

[20] T. Ramstad, P. E. Øren, and S. Bakke, "Simulation of two-phase flow in reservoir rocks using a lattice Boltzmann method," *SPE Journal*, vol. 15, no. 4, pp. 917–927, 2010.

[21] C. Y. Lin, Y. Q. Wu, L. H. Ren et al., "Review of digital core modeling methods," *Progress in Geophysics*, vol. 33, pp. 679–689, 2018.

[22] H. J. Vogel and K. Roth, "Quantitative morphology and network representation of soil pore structure," *Advances in Water Resources*, vol. 24, no. 3-4, pp. 233–242, 2001.

[23] C. H. Arns, F. Bauget, A. Limaye et al., "Pore-scale characterization of carbonates using X-ray microtomography," *SPE Journal*, vol. 10, no. 4, pp. 475–484, 2005.

[24] J. Zhao, L. Cui, H. Chen, N. Li, and Z. Wang, "Quantitative characterization of rock microstructure of digital core based on CT scanning," *Geoscience*, vol. 34, pp. 1205–1213, 2020.

[25] L. Sun, X. Wang, X. Jin, J. Li, and S. Wu, "Three dimensional characterization and quantitative connectivity analysis of micro/nano pore space," *Petroleum Exploration and Development*, vol. 43, no. 3, pp. 537–546, 2016.

[26] J. A. Quiblier, "A new three-dimensional modeling technique for studying porous media," *Journal of Colloid and Interface Science*, vol. 98, pp. 84–102, 1984.

[27] R. D. Hazlett, "Statistical characterization and stochastic modeling of pore networks in relation to fluid flow," *Mathematical Geology*, vol. 29, no. 6, pp. 801–822, 1997.

[28] K. Wu, M. I. Van Dijke, G. D. Couples et al., "3D stochastic modelling of heterogeneous porous media - applications to reservoir rocks," *Transport in Porous Media*, vol. 65, no. 3, pp. 443–467, 2006.

[29] Y. Wu, C. Lin, L. Ren et al., "Digital core modeling based on multiple-point statistics," *Journal of China University of Petroleum*, vol. 42, no. 3, pp. 12–21, 2018.

[30] P. E. Øren and S. Bakke, "Process based reconstruction of sandstones and prediction of transport properties," *Transport in Porous Media*, vol. 46, no. 2/3, pp. 311–343, 2002.

[31] N. Alqahtani, F. Alzubaidi, R. T. Armstrong, P. Swietojanski, and P. Mostaghimi, "Machine learning for predicting properties of porous media from 2d X-ray images," *Journal of Petroleum Science and Engineering*, vol. 184, article 106514, 2020.

[32] M. Misbahuddin, "Estimating petrophysical properties of shale rock using conventional neural networks CNN," in *Proceedings-SPE Annual Technical Conference and Exhibition*, 2020.

[33] D. J. Rezende, S. Mohamed, and D. Wierstra, "Stochastic backpropagation and approximate inference in deep generative models," *Proceedings of the 31st International Conference on Machine Learning*, vol. 32, no. 2, pp. 1278–1286, 2014.

[34] I. J. Goodfellow, J. Pouget-Abadie, M. Mirza et al., "Generative adversarial nets," *Advances in Neural Information Processing Systems*, vol. 3, pp. 2672–2680, 2014.

[35] L. Mosser, O. Dubrule, and M. J. Blunt, "Reconstruction of three-dimensional porous media using generative adversarial neural networks," *Physical Review E*, vol. 96, no. 4, 2017.

[36] L. Mosser, O. Dubrule, and M. J. Blunt, "Stochastic reconstruction of an oolitic limestone by generative adversarial networks," *Transport in Porous Media*, vol. 125, no. 1, pp. 81–103, 2018.

[37] A. Valsecchi, S. Damas, C. Tubilleja, and J. Arechalde, "Stochastic reconstruction of 3D porous media from 2D images using generative adversarial networks," *Neurocomputing*, vol. 399, pp. 227–236, 2020.

[38] W. Zha, X. Li, Y. Xing, L. He, and D. Li, "Reconstruction of shale image based on Wasserstein generative adversarial networks with gradient penalty," *Advances in Geo-Energy Research*, vol. 4, no. 1, pp. 107–114, 2020.

[39] J. Feng, X. He, Q. Teng, C. Ren, H. Chen, and Y. Li, "Reconstruction of porous media from extremely limited information using conditional generative adversarial networks," *Physical Review E*, vol. 100, no. 3, article 33308, 2019.

[40] D. Volkhonskiy, E. Muravleva, O. Sudakov et al., "Reconstruction of 3D porous media from 2D slices," 2019, https://arxiv.org/pdf/1901.10233.pdf.

[41] T. Zhang, D. Li, and F. Lu, "A pore space reconstruction method of shale based on autoencoders and generative adversarial networks," *Computational Geosciences*, vol. 25, no. 6, pp. 2149–2165, 2021.

[42] J. Feng, Q. Teng, B. Li, X. He, H. Chen, and Y. Li, "An end-to-end three-dimensional reconstruction framework of porous media from a single two-dimensional image based on deep learning," *Computer Methods in Applied Mechanics and Engineering*, vol. 368, article 113043, 2020.

[43] Y. Wang, C. H. Arns, S. S. Rahman, and J. Y. Arns, "Porous structure reconstruction using convolutional neural networks," *Mathematical Geosciences*, vol. 50, no. 7, pp. 781–799, 2018.

[44] Y. Z. Ong, N. You, and Y. E. Li, "Digital rock image inpanting using GANs," *SEG International Exposition and 90th Annual Meeting*, vol. 2020, pp. 2525–2529, 2020, segam2020-3427515.1.

[45] A. Radford, L. Metz, and S. Chintala, "Unsupervised representation learning with deep convolutional generative adversarial networks," 2015, https://arxiv.org/abs/1511.06434.

[46] H. Dong and M. J. Blunt, *Micro-CT Imaging and Pore Network Extraction [Ph.D. Thesis]*, Earth science and engeneering, 2007.